NMR Investigation of Primer-Template Models: Structural Effect of Sequence Downstream of a Thymine Template on Mutagenesis in DNA Replication†

Lai Man Chi and Sik Lok Lam*

Department of Chemistry, The Chinese University of Hong Kong, Shatin, New Territories, Hong Kong

Received May 7, 2007; Revised Manuscript Received June 8, 2007

ABSTRACT: Misaligned structures can occur in primer-templates during DNA replication, which can be bypassed and extended by low-fidelity polymerases and ultimately lead to mutations. In this study, we have investigated how the nucleotide downstream of a thymine template affects the primer-template structures upon misincorporation of dNTPs. The base pair structures at the replicating sites of a set of primer-template models containing either a G or an A downstream of the thymine template have been determined using NMR spectroscopy. Incorporation of dCTP and dTTP opposite 5′-GT and 5′-AT templates, respectively, can result in misaligned structures with a T-bulge. Depending on the downstream sequence, subsequent extension of the primers may stabilize the misaligned structures or cause the formation of mismatched structures. These results provide alternative pathways for base substitution and deletion errors during DNA replication by low-fidelity polymerases.

Replication fidelity of DNA has been extensively studied in the past several decades, and it is well accepted that the fidelity is related to selectivity of DNA polymerase, exonucleolytic proofreading function, and post-replication mismatch repair activity (*1*). Highly processive and accurate DNA synthesis is required for maintaining genetic information and avoiding mutations that can initiate and promote human diseases over generations. On the contrary, mutations resulting from uncorrected errors during DNA synthesis are essential to facilitate translesion synthesis of otherwise replication-blocking lesions. They are counterbalanced by the requirement for mutations in evolution, fitness, and immunological diversity (*2*).

Recent discovery of the proofreading deficient Y-family DNA polymerases provide new mechanistic pathways for evolution by efficiently bypassing damaged template of bulky DNA adducts and/or replicating undamaged DNA with a 10- to 100-fold increase in error rate compared to other family polymerases (*3*−*7*). The Y-family polymerases have no detectable sequence similarity with other family polymerases and lack any intrinsic exonucleolytic activity for proofreading (*8*). Their shapes resemble a right hand with fingers, palm, thumb, and a unique C-terminal little finger domain (*9*, *10*). Unlike other family polymerases, their active sites are open and spacious such that only a few van der Waals contacts are present with the replicating base pairs. Thereby, bulky adducts, wobble or Hoogsteen base pairs are allowed at or beyond the loose active site (*11*−*13*). Recently, it has been demonstrated that a single-nucleotide bulge formed at the template terminus could be extended by a low-fidelity polymerase (*14*). In addition, crystal structures of a low-fidelity polymerase containing a misaligned DNA template in active sites have been determined (*12*, *15*). These results show that the formation and accommodation of a misaligned primer-template in the loose active site is possible (*16*), which ultimately can lead to dislocation mutagenesis (*17*−*19*). Yet whether misalignment of primer-template is due to the presence of the polymerase or template sequence remains elusive.

Slipped frameshift intermediates can occur when the polymerase slows or stalls at sites of lesions during DNA replication (*20*−*26*). However, such effects are much less common when unmodified DNA is replicated. Recently, NMR[1] structural investigation has been performed on primer-template oligonucleotide models which mimic the situation that a dGTP has just been incorporated opposite a 5′-CT template (*27*), revealing the occurrence of misaligned primer-template structure (Figure 1a). Depending on the sequence downstream of the 5′-CT, further extension of the primer can lead to realignment and ultimately the formation of a G•T mismatch. In addition to direct incorporation of G opposite T, this provides an alternative mechanistic pathway for G•T wobble pair formation in the loose active center of the human Y-family polymerase Pol*ι* (*13*), explaining why insertion of dGTP opposite a thymine template is even more efficient than insertion of A opposite T (*28*−*30*).

In this study, we have investigated how the nucleotide downstream of the thymine template affects the alignment of primer-templates. The base pair structures at replicating sites of a set of primer-template models containing either a G (Figure 1b) or an A (Figure 1c) downstream of the thymine template have been determined using NMR spectroscopy.

† The work described in this paper was fully supported by a grant from the Research Grants Council of the Hong Kong Special Administrative Region (Project No. CUHK401107).

* To whom correspondence should be addressed. Phone: (852) 2609-8126. Fax: (852) 2603-5057. E-mail: lams@cuhk.edu.hk.

[1] Abbreviations: NMR, nuclear magnetic resonance; dNTP, deoxyribonucleoside triphosphate; NOE, nuclear Overhauser effect; 2D NOESY, two-dimensional nuclear Overhauser effect spectroscopy; pol*ι*, polymerase iota; DSS, 2,2-dimethyl-2-silapentane-5-sulfonic acid; WATERGATE, water suppression by gradient-tailored excitation.

10.1021/bi700865e CCC: $37.00
Published on Web 07/21/2007

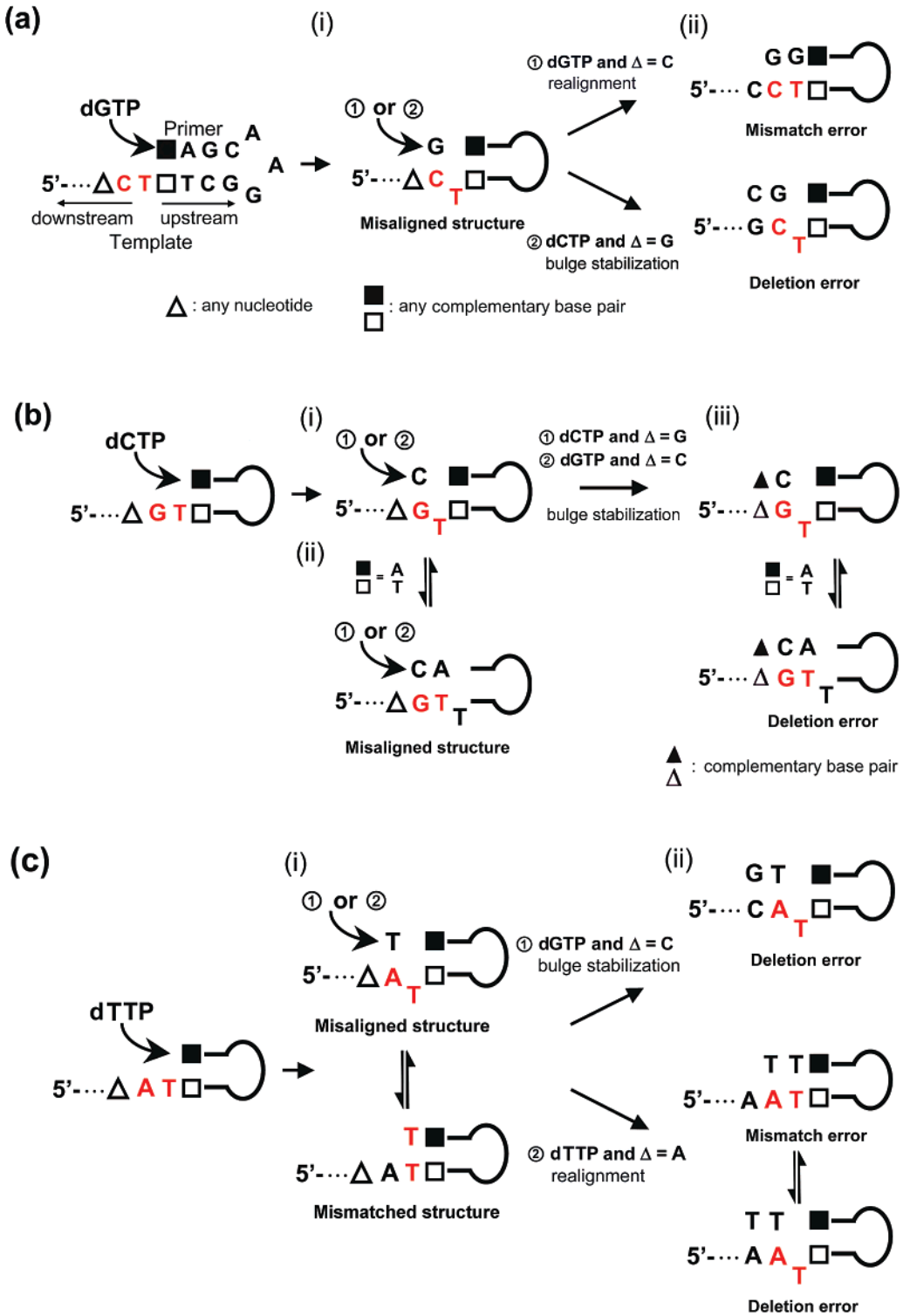

FIGURE 1: (a) (i) For a 5′-CT template, misalignment leads to the formation of a G·C base pair and a T-bulge. (ii) Further synthesis on the misaligned sample can bring about either mismatch or deletion errors. All primer-template models were designed to form a hairpin with a 5′-GAA loop. The top and bottom strands mimic the primer and template, respectively. (b) (i) For a 5′-GT template, misalignment also occurs, leading to the formation of a C·G base pair and a T-bulge. (ii) Rearrangement of the bulge position occurs when the nucleotide upstream of 5′-GT is T. (iii) Further synthesis on the misaligned sample can bring about deletion error. (c) (i) For a 5′-AT template, both misaligned and mismatched conformers are formed upon incorporation of dTTP. (ii) Further synthesis can lead to either mismatch or deletion errors.

We have demonstrated that misaligned structures containing a T-bulge may be formed upon incorporation of dCTP and dTTP opposite 5′-GT and 5′-AT templates, respectively. Based on the sequence downstream of these templates, subsequent primer extension may either stabilize the misaligned structures or cause the formation of mismatched structures, which ultimately leads to deletion and base substitution errors, respectively.

MATERIALS AND METHODS

Sample Design. All DNA samples were designed to form a hairpin with the top and bottom strands mimicking the

primer and template, respectively (Figure 1). The 5′-GAA hairpin loop (*31*) serves as a linker to connect the upper primer and lower template strands together in order to simplify the sample preparative work. These samples mimic the primer-templates that a dNTP has just been incorporated into templates. The 5′-overhang region of the samples represents the template sequences whereas the 3′-terminal nucleotide represents the newly incorporated dNTP at the end of primers.

Sample Preparation. All DNA samples were synthesized using an Applied Biosystems model 392 DNA synthesizer and purified using denaturing polyacrylamide gel electrophoresis and diethylaminoethyl Sephacel anion exchange column chromatography. NMR samples were prepared by dissolving 0.5 μmol of purified DNA samples into 500 μL of buffer solution containing 150 mM sodium chloride, 10 mM sodium phosphate at pH 7.0, and 0.1 mM DSS.

NMR Analysis. All NMR experiments were performed using either a Bruker ARX-500 or AV-500 spectrometer operating at 500.13 MHz and acquired at 25 °C unless stated otherwise. For studying the resonance signals from labile protons, the samples were prepared in 90% H_2O/10% D_2O buffer solution. 1D imino proton spectra were acquired using WATERGATE pulse sequence (*32*, *33*), and 2D WATERGATE-NOESY experiments were performed at 300 ms mixing time. For studying nonlabile proton signals, the solvent was exchanged to 100% D_2O solution. 2D NOESY experiments were also performed at 300 ms mixing time, and 4k × 512 data sets were collected. The acquired data were zero-filled to give 4k × 4k spectra with cosine window function applied to both dimensions.

RESULTS

In this study, solution base pair structures at the replicating sites of 5′-GT and 5′-AT templates were determined after the incorporation of dCTP and dTTP, respectively. High-resolution NMR spectroscopic investigations focusing on 1D imino proton and 2D NOESY analysis were performed to probe the replicating site structures of the primer-template models. The appearance of imino proton signal indicates that the rate of exchange with solvent is slow on the NMR time scale. For Watson−Crick base pairs, the imino signals usually show up in the 12−14 ppm region, whereas imino signals arising from unpaired bases or mispairs usually appear more upfield. On the other hand, the presence of a NOE cross-peak between two protons in different nucleotides indicates that the two nucleotides are in proximity to each other. Sequential proton resonance assignments were made by investigating the fingerprint regions in 2D NOESY and WATERGATE-NOESY spectra (Supporting Information, S1−S7).

Incorporation of a dCTP Opposite a 5′-GT Template. When dCTP was incorporated opposite a 5′-GT template sequence, a C·G Watson−Crick base pair and a T-bulge were formed due to misalignment (Figure 2a). This was supported by the presence of an unusual G2H1′−G4H8 NOE (Figure 2b), which indicates that G2 and G4 are close in space. In regular B-DNA duplexes, it is expected that sequential connectivities between consecutive nucleotides would be present in the 2D NOESY spectrum (*34*). No G2H1′−T3H6 and T3H1′−G4H8 NOEs were observed in this case, further supporting that the primer-template was misaligned. Moreover, the presence of a G2 imino signal at lower temperatures reveals the presence of a C15·G2 Watson−Crick base pair (Figure 2b), confirming that the primer-template was misaligned.

Upon further extending the primer with a G opposite C downstream of the 5′-GT template, the T-bulge of the misaligned structure was stabilized as supported by a G2−G4 NOE and a G2 imino signal at 25 °C (Figure 2c). This is further supported by the appearance of a G16 imino at 5 °C, confirming the presence of a G16·C1 base pair. As realignment has been observed on a 5′-CT template (*27*), it will be interesting to see if such realignment would also occur on a 5′-GT template. When the nucleotide downstream of the 5′-GT template was a G, the misaligned structure was also stabilized upon extending with a C. No realignment leading to the formation of the C15·T3 mispair and C16·G2 base pair was observed as evidenced by the G2−G4 NOE and the presence of G1 and G2 imino signals (Figure 2d).

To investigate if the base pair upstream of the 5′-GT template affects the misalignment process, we substituted a C14·G4 base pair with T14·A4 and G14·C4, respectively. In both cases, the template strands were also slipped, leading to misalignment as supported by their NOESY and imino proton spectra (Supporting Information, S8). The presence of a NOE between the second and fourth nucleotides and G2 imino signals confirmed these misaligned structures.

The slippage process became more complicated when C14·G4 was substituted with A14·T4 because this brought about three consecutive Ts, i.e., T3, T4, and T5, in the template sequence (Figure 3a). It is now possible that the T-bulge in position 3 (T3-conformer) of the misaligned structure can be rearranged to position 4 (T4-conformer) and/or position 5 (T5-conformer). Only a single set of imino signals was observed at 25 °C (Figure 3a), suggesting the presence of (i) only one conformer or (ii) multiple conformers which undergo rapid exchange. The appearance of G2−T4, G2−T3, and T3−T4 NOEs at 25 °C does not support the presence of only one conformer. Instead, it provides evidence for the presence of T3-, T4-, and T5-conformers. At 5 °C, all three conformers are present as evidenced by the appearance of five G imino signals (Figure 3a). If only a single conformer were present, only three G imino signals would be observed. Therefore, G2−T4, G2−T3, and T3−T4 NOEs resulted from the averaged structure of the weighted population of these three conformers. Owing to the more intense G2−T4 NOE when compared to G2−T3 and T3−T4 NOEs, it is believed that the predominant species is the T3-conformer at 25 °C.

In order to determine if rearrangement of T-bulge positions would lead to realignment upon primer extension, we extended the primer with a C opposite G downstream of the 5′-GT template as shown in Figure 3b. The presence of G1 and G2 imino signals at 25 °C indicates that there are C16·G1 and C15·G2 base pairs, confirming that no realignment occurs upon primer extension. The appearance of only one set of G imino and G2−T4, G2−T3, and T3−T4 NOEs suggests the presence of T3-, T4-, and T5-conformers which undergo rapid exchange. The more intense G2−T4 and G2−T3 NOEs when compared to the T3−T4 NOE indicate T3- and T4-conformers are predominant. The exchange between these two conformers remains rapid at 5 °C as no additional G imino signal was observed. The presence of only one

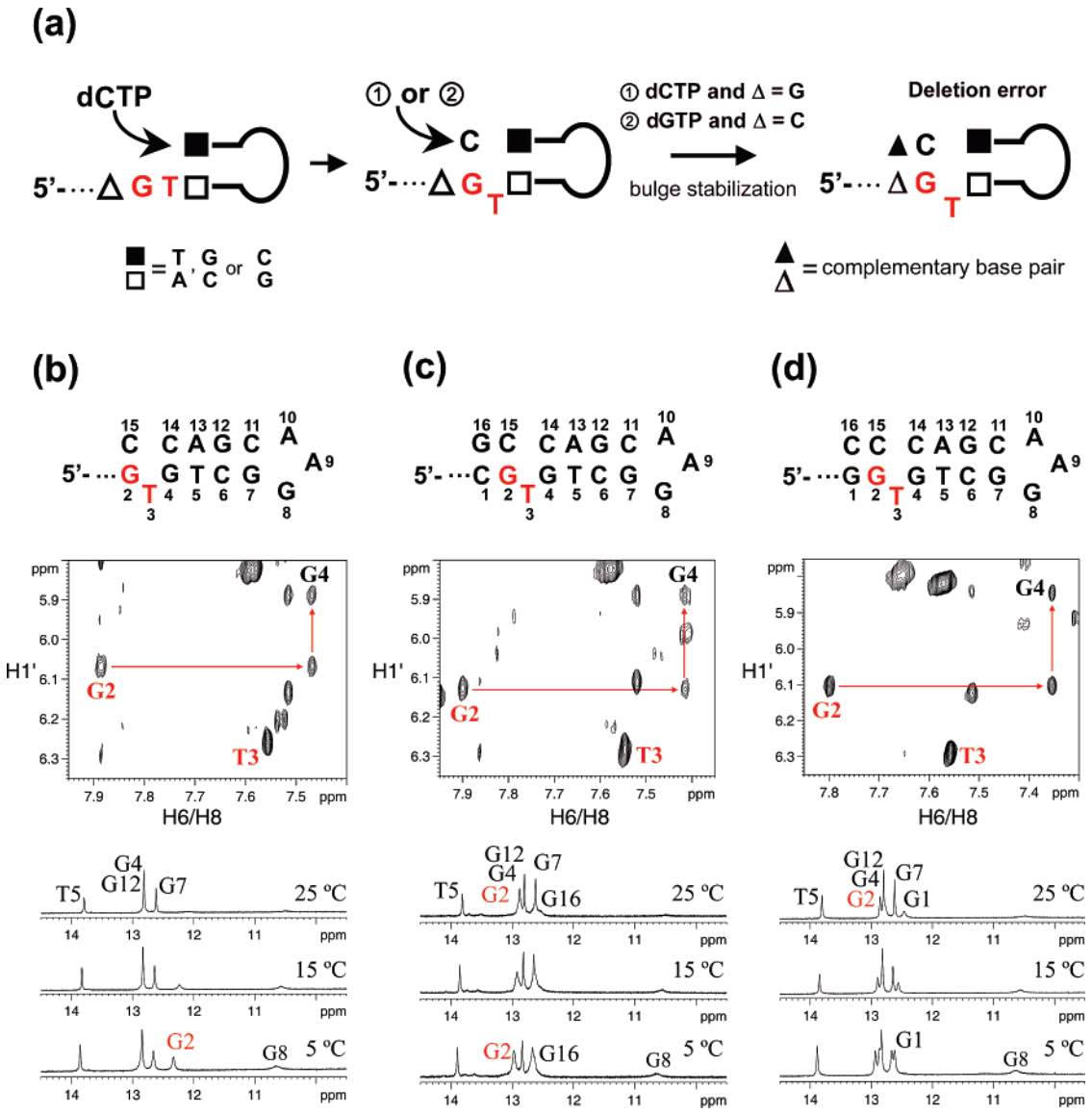

FIGURE 2: NMR evidence for misaligned structures. (a) Misaligned structure formed after incorporation of a dCTP opposite a 5′-GT template.(b) The NOESY H6/H8−H1′ fingerprint region shows an unusual cross-peak between G2 and G4. The presence of a G2 imino signal at 5 °C shows that there is a C15·G2 Watson−Crick base pair. The small signal at about 10.7 ppm corresponds to the G8 imino of a sheared G·A mispair in the GAA loop. (c) The same NOESY region of the primer-template shows a G2−G4 NOE after further extension with a G opposite C downstream of the 5′-GT template. The imino signals of G2 and G16 indicate the presence of C15·G2 and G16·C1 Watson−Crick base pairs. (d) Further extension with a C opposite G downstream of the 5′-GT template, G2−G4 NOE was also observed in the same NOESY region of the primer-template. The imino signal of G2 and G1 indicates the presence of C15·G2 and C16·G1 Watson−Crick base pairs.

observable weak and broad thymine signal, which is due to T5 of the T3-conformer, also supports this exchange process.

Incorporation of a dTTP Opposite a 5′-AT Template. Apart from the 5′-CT (*27*) and 5′-GT templates, we have also investigated the primer-template structure after incorporation of a dTTP opposite a 5′-AT template (Figure 1c). Owing to the chemical shift of T imino in the T·A base pair being about 14 ppm (*35*) and that of a T·T mispair being about 10.5 ppm (*36*) in regular B-DNA helix, the small imino peak near 12 ppm at 5 °C (Figure 4a) was assigned to the averaged T15 imino signals from T15·A2 of the misaligned conformer and T15·T3 of the mismatched conformer, suggesting the presence of both conformers which undergo rapid exchange. Similarly, the small and broad imino signal near 11 ppm in Figure 4a was due to the averaging of T3 imino signals from the T-bulge of the misaligned conformer and T3·T15 mispair of the mismatched conformer (Supporting Information, S9). The appearance of A2−G4, A2−T3, and T3-G4 NOEs (Figure 4a) also supports the presence of the two conformers, with the first NOE biased toward the misaligned form and the latter two biased toward the mismatched form.

In order to investigate whether the flanking base pair upstream of 5′-AT template would affect the primer-template structures after incorporation of a dTTP, we substituted C14·G4 with G14·C4 and T14·A4, respectively (Supporting Information, S10). Similar results were observed in both samples, indicating the presence of both misaligned and mismatched conformers, and they undergo rapid exchange. When C14·G4 was substituted with A14·T4, three consecutive Ts would be present in the template strand (Figure 4b). Unlike the situation with 5′-GT template, the T-bulge in the misaligned form did not rearrange from position 3 to other positions as evidenced by the appearance of T4 imino signal which indicates the presence of the A14·T4 base pair. Owing

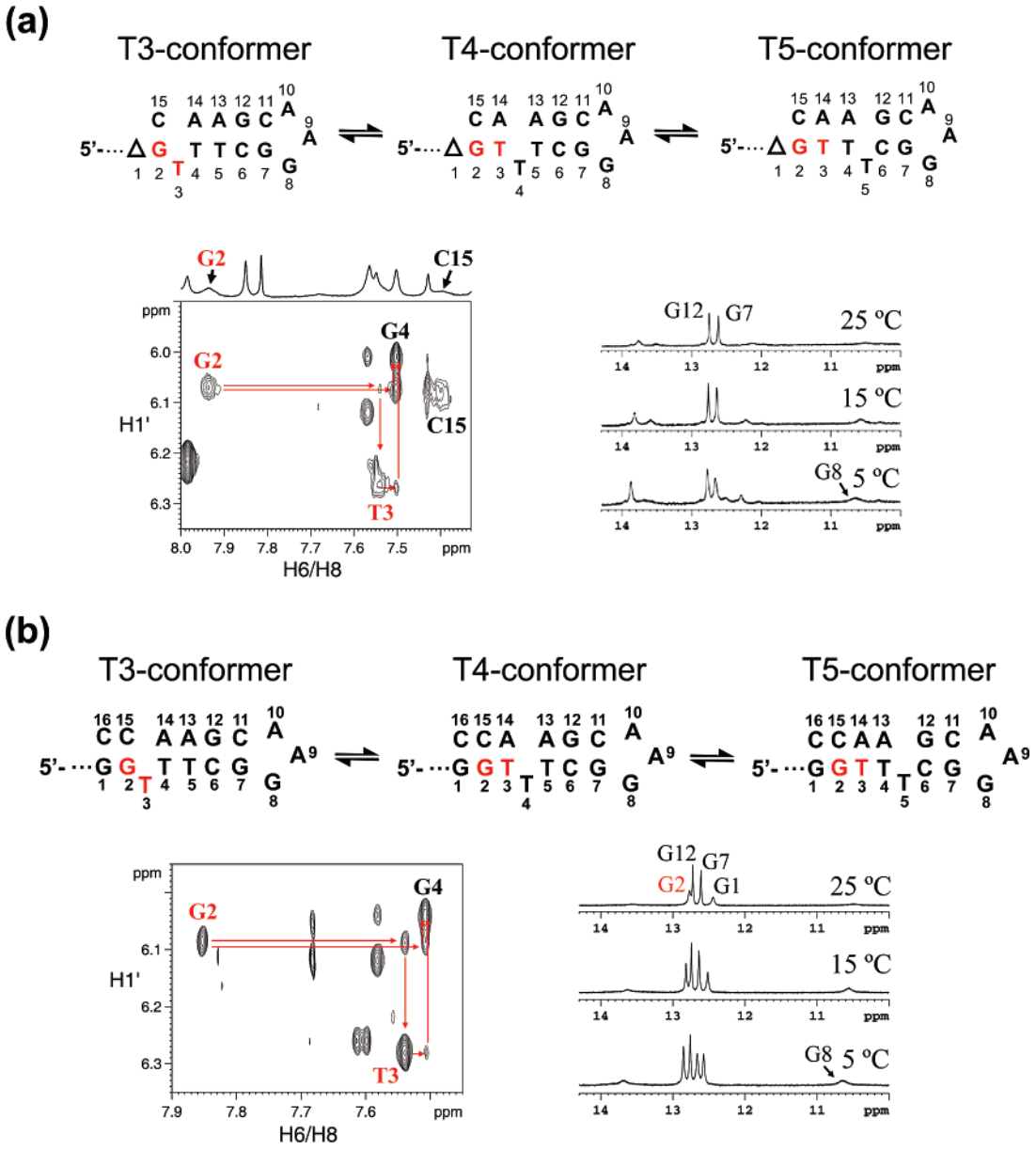

FIGURE 3: (a) Rearrangement of the T-bulge position occurs when the nucleotide upstream of 5′-GT is T, leading to three possible conformers. NOEs and imino signals at lower temperatures show the presence of three conformers. At 5 °C, the small signal at about 10.7 ppm corresponds to the G8 imino of a sheared G·A mispair in the GAA loop. The red arrows indicate the sequential NOE connectivities corresponding to the conformers. (b) Addition of a C·G base pair does not stop the rearrangement of the T-bulge position.

to the similar H1′ chemical shifts of A2 and T3, there are probably spectral overlaps between A2H1′−T4H6 and T3H1′−T4H6 NOEs, and A2H1′−T3H6 and T3H1′−T3H6 NOEs. We attempted to resolve these NOEs at 10 °C but without success. Nevertheless, the presence of both misaligned and mismatched conformers were supported by the small imino signal near 11.5 ppm that is due to the averaging of T15 imino signals from the T15·A2 base pair and the T15·T3 mispair, as well as the small imino signal near 11 ppm that is due to the averaging of T3 imino signals from the T-bulge and the T3·T15 mispair.

Further extending the primer with a G opposite C downstream of the 5′-AT template resulted in a single misaligned conformer. The presence of an A2−G4 NOE suggests a T-bulge in position 3 whereas the presence of T15 and G16 imino signals confirms T15·A2 and G16·C1 base pairs (Figure 4c). In addition, A2−T3 and T3−G4 NOEs were not observed, indicating that there is no mismatched conformer. On the contrary, addition of a T·A Watson−Crick base pair did not hamper the formation of mismatched conformer. The small and broad imino signal near 12 ppm (Figure 4d) due to the averaging of T15 imino signals from a T15·A2 base pair and a T15·T3 mispair reveals the presence of both misaligned and mismatched conformers, which undergo rapid exchange. This peak was further broadened at 5 °C, indicating moderate exchange between the two conformers. The appearance of A2−G4, A2−T3, and T3−G4 NOEs at 5 °C also agrees well with the averaged structure between the misaligned and mismatched conformers (Figure 4d).

The conformational exchange process became slow at 5 °C after adding another T·A base pair. At this temperature, no averaging of T15 imino signals of the two conformers was observed (Figure 4e). The small T16 and T15 imino signals near 14 ppm belong to T16·A1 and T15·A2 of the misaligned conformer, respectively. Due to end-fraying of

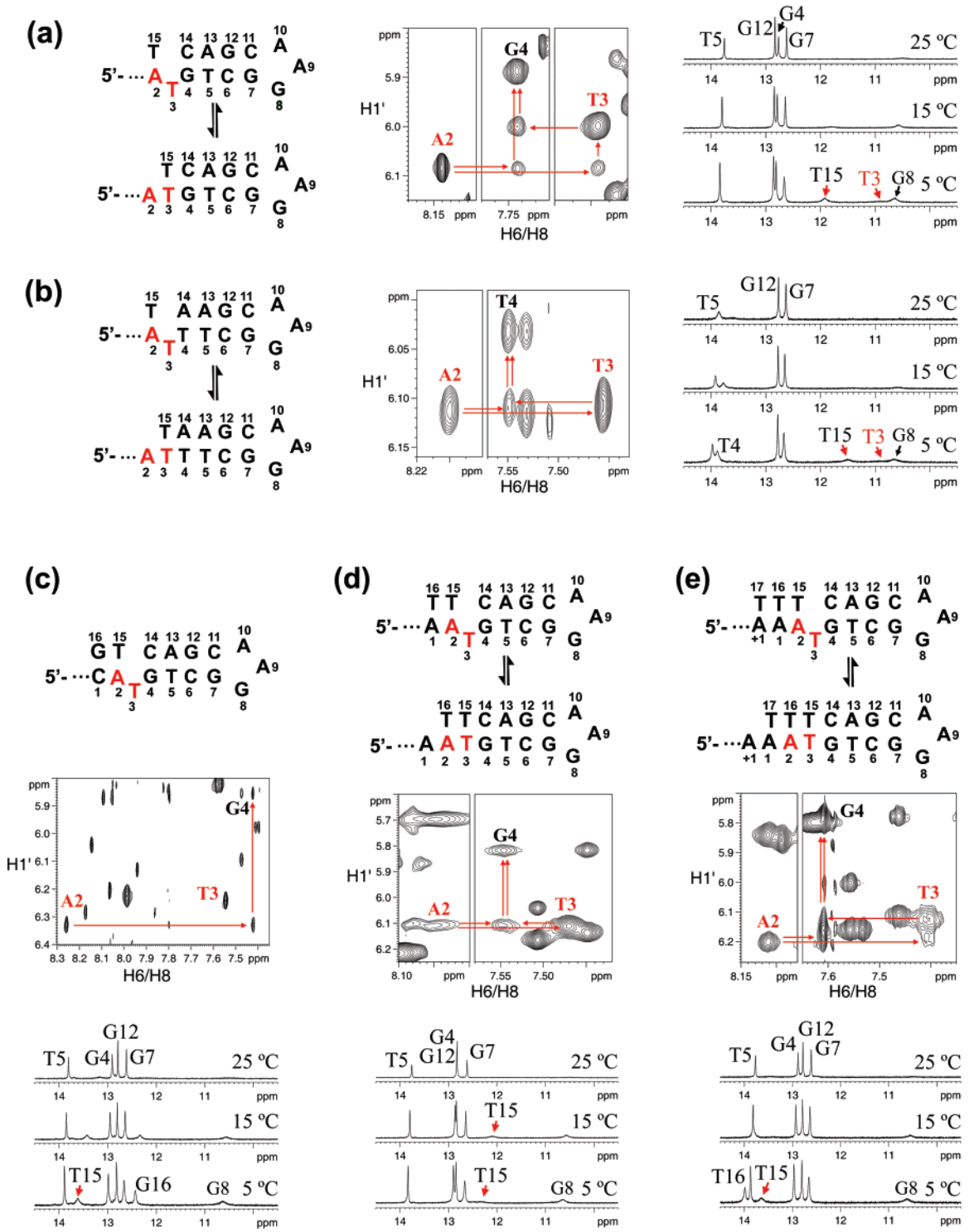

FIGURE 4: (a) Both misaligned and mismatched conformers are present upon incorporation of a dTTP opposite a 5′-AT template. The small T3 and T15 imino signals near 11 and 12 ppm at 5 °C, respectively, indicate rapid exchange of the two conformers. The small signal at about 10.7 ppm corresponds to the G8 imino of a sheared G·A mispair in the GAA loop. The red arrows indicate the sequential NOE connectivities corresponding to the conformers. (b) For a 5′-AT template, there is no rearrangement of the T-bulge position. (c) Addition of a G·C Watson−Crick base pair stabilizes the misaligned conformer and stops the exchange with the mismatched conformer. (d) Instead, addition of a T·A base pair does not stop the conformational exchange. (e) Further addition of another T·A base pair slows down the exchange between the two conformers.

the terminal T17·A+1 base pair of the misaligned conformer, a T17 imino signal was not observed. In addition, T15·T3 imino signals from the mismatched conformer were also not observed at 5 °C probably due to its lower thermodynamic stability than T·A base pair. Nevertheless, the presence of A2−G4, A2−T3, and T3−G4 NOEs at 5 °C (Figure 4e) and 25 °C (Supporting Information, S11) supports the presence of both the misaligned and mismatched conformers.

DISCUSSION

Rearrangement of T-Bulge in Misaligned Conformers. For the 5′-GT template with an upstream nucleotide T, upon

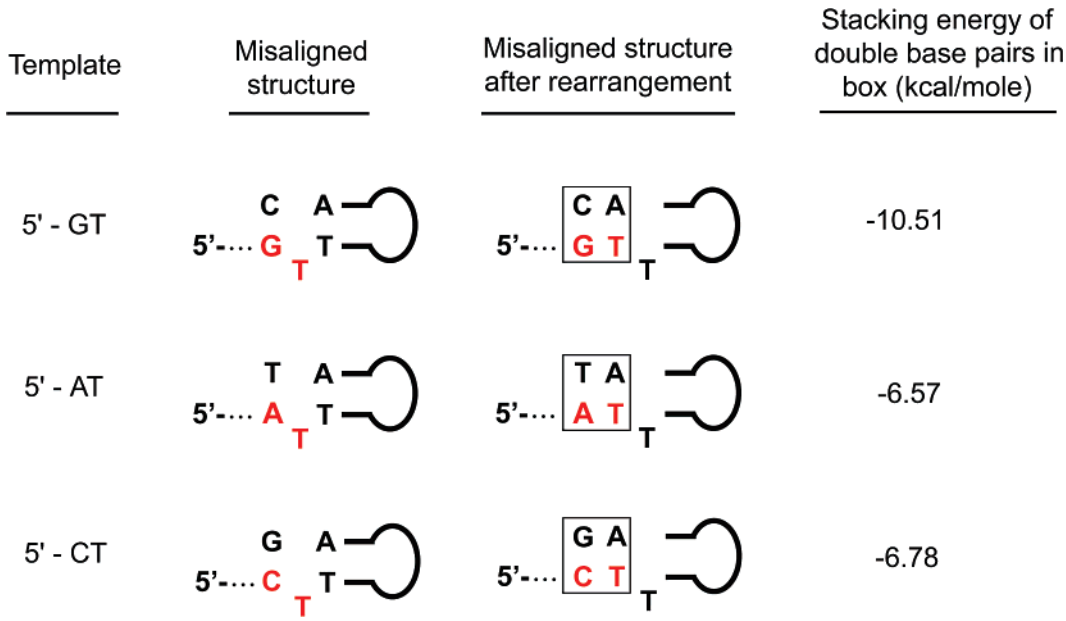

FIGURE 5: Stacking energy difference after rearrangement of the T-bulge position in the misaligned structures. The stacking energies were calculated for the double base pairs indicated by a box.

incorporation of a dCTP, rearrangement of the T-bulge from position 3 to positions 4 and 5 was observed (Figure 3a). This rearrangement was only observed in the 5′-GT template but not in 5′-CT (*27*) and 5′-AT templates. In order to understand the chemical forces governing this process, we compared the thermodynamic stabilities of the conformers after rearranging the T-bulge from position 3 to 4 (Figure 5). Among these conformers, the only difference was the double base pairs downstream of the T-bulge (Figure 5). By comparing the stacking energy of the double base pairs from literature (*37*), the stacking energy difference between the 5′-GT and 5′-CT structures was equal to the difference in the stacking energy of their corresponding double base pairs, i.e., $-(10.51 - 6.78) = -3.73$ kcal/mol. Similarly, the stacking energy difference between the 5′-GT and 5′-AT structures was found to be −3.94 kcal/mol. These values indicate that the misaligned form of 5′-GT template after rearrangement is ∼4 kcal/mol more stable than the other two misaligned conformers, suggesting that rearrangement of T-bulge positions is driven by the stabilizing interactions resulting from the double base pairs.

By comparing the imino proton spectra at 5 °C in Figures 3a and 3b, the rate of T-bulge rearrangement was found to be faster after primer extension in the 5′-GT template. The presence of prominent end-fraying before primer extension, as evidenced by the broad G2 and C15 signals in Figure 3a, is likely to be the major cause that slows down the T-bulge rearrangement process. On the contrary, end-fraying became less serious upon adding a C·G base pair which stacked on the base pair downstream of the T-bulge and thereby the rate of T-bulge rearrangement became faster.

Mismatch Formation in 5′-CT, 5′-AT, and 5′-GT Templates. For the 5′-CT template, a G·T mismatch was found to occur via realignment of misaligned structure upon primer extension (*27*). For the 5′-AT template, our results suggest that a T·T mismatch may occur via direct incorporation of T opposite a thymine template or realignment of misaligned structure. Further primer extension is not required to yield a T·T mismatch. For the 5′-GT template, a C·T mismatch formation was not observed either before or after further primer extension. Since thermodynamic stabilities of these mismatches follow the order G·T > T·T > C·T (*36*, *38*, *39*), we believe that the formation propensity of these mismatches during DNA replication is related to their stabilities.

Factors Affecting Misalignment. It is believed that misalignment leading to bulge formation is always unfavorable due to its destabilizing effect on the base pairing and stacking of neighboring base pairs. However, misalignment could still occur since the stabilizing effect owing to the formation of Watson−Crick base pair outweighs the destabilizing T-bulge. In this study, we showed that G·C and C·G base pairs have a larger stabilizing effect on the misaligned structure than the A·T base pair. Therefore, the formation of a T-bulge is more likely if the misincorporation of nucleotide opposite template can cause template slippage to form a G·C or C·G base pair. If the newly formed base pair is A·T, the misaligned structure is probably not stable, leading to the coexistence of misaligned and mismatched conformers.

Misincorporation of dGTP opposite a 5′-CT template can lead to misalignment, and the nucleotide downstream of a 5′-CT template has been found to be critical to determine if realignment of the misaligned structure would occur (*27*). Similarly, the present study also shows the importance of the sequence downstream of 5′-GT and 5′-AT templates. Although the consequences after incorporation of a dNTP depend on the type of incoming dNTP and the template sequence, all four types of dNTP have equal chances to be added to the primer. Therefore, the template sequence, on one hand, participates as a passive substrate in the replication process, but, on the other hand, it also plays an active structural role in governing the formation of misaligned structures and thereby determining the type of mutations.

Biological Implications of Misincorporation on Thymine Template. In this study, we investigated the base pair structures at replicating sites of primer-template models, which mimic the situation after a misincorporation of dNTP opposite a thymine template. Together with our previous

results on 5′-CT template (*27*), we demonstrated that if the template sequence T is followed by C, G, or A, it is possible that incorporation of an incorrect dNTP can cause misalignment of primer-template, leading to the formation of a T-bulge. Upon further primer extension, we found that misaligned structure can (i) further be stabilized, (ii) realign to form a mismatched conformer, or (iii) exchange with a mismatched conformer. Depending on the template sequence further downstream, subsequent incorporation of dNTPs can lead to either mismatch or deletion error. In addition, the template sequence will also affect the exchange rate between the misaligned and mismatched conformers as shown in the case of 5′-AT template in this study.

In order to simplify the sample preparative work, a single strand of hairpin sequences was used to mimic primer-templates instead of two longer strands of DNA sequences. Owing to the formation of sheared G·A mispair in the 5′-GAA loop which stabilizes the hairpin structures (*31*), the stem regions of the hairpin models were expected to behave similarly to B-DNA double helices. The proton chemical shifts of nucleotides in the stem region except the loop closing base pair agree well with the predicted shifts of B-DNA (*35*, *40*), indicating that the hairpin stem structure is very similar to B-DNA double helices. Therefore, the results of this work are also applicable to DNA primer-templates with longer sequences.

Crystallographic studies have shown that the spacious active site of low-fidelity polymerase is capable of accommodating a misaligned DNA template (*12*, *15*). In addition, it has also been shown that primer extension by low-fidelity polymerase on a single-nucleotide bulge formed at the template terminus is possible (*14*). As a consequence, the errors resulting during DNA replication by low-fidelity polymerase may be related to the propensity of the template forming misaligned structures. The findings here relate to the thermodynamics of isolated DNA primer-template models. Since individual DNA polymerases are likely to interact with primer-template DNA differently, the extent to which these structures occur in DNA polymerases may also depend upon the specific polymerase in question. Additional structural investigations have to be performed to provide a clear picture on the misaligned structure formation propensity of different sequences. Then, statistical analysis can be carried out to study the relationship of template sequence and mutation hotspots during DNA replication by low-fidelity polymerases.

CONCLUSIONS

The present work reveals the effects of the templating bases leading to misaligned structures in primer-templates. Our results suggest alternative pathways for mutations to occur during DNA replication by low-fidelity polymerases. It is possible that base substitution and frameshift mutations are determined by template sequences. In order to investigate the mechanistic pathways for the occurrence of mutations during low-fidelity DNA replication, further investigation is needed to determine whether misalignment occurs at time scales faster than the rate at which a second nucleotide is incorporated.

ACKNOWLEDGMENT

We would like to thank C. K. Kwok, F. K. Lo, and H. Yang for preparing some of the DNA samples in this study.

SUPPORTING INFORMATION AVAILABLE

Figures showing sequential assignment, NOESY and imino proton spectra of the primer-templates. This material is available free of charge via the Internet at http://pubs.acs.org.

REFERENCES

1. Kunkel, T. A. (2004) DNA replication fidelity, *J. Biol. Chem. 279*, 16895−16898.
2. Tippin, B., Pham, P., and Goodman, M. F. (2004) Error-prone replication for better or worse, *Trends Microbiol. 12*, 288−295.
3. Goodman, M. F. (2002) Error-prone repair DNA polymerases in prokaryotes and eukaryotes, *Annu. Rev. Biochem. 71*, 17−50.
4. Johnson, R. E., Washington, M. T., Prakash, S., and Prakash, L. (2000) Fidelity of human DNA polymerase *η*, *J. Biol. Chem. 275*, 7447−7450.
5. Johnson, R. E., Prakash, S., and Prakash, L. (2000) The human DINB1 gene encodes the DNA polymerase Pol*θ*, *Proc. Natl. Acad. Sci. U.S.A. 97*, 3838−3843.
6. Ohashi, E., Bebenek, K., Matsuda, T., Feaver, W. J., Gerlach, V. L., Friedberg, E. C., Ohmori, H., and Kunkel, T. A. (2000) Fidelity and processivity of DNA synthesis by DNA polymerase *κ*, the product of the human DINB1 gene, *J. Biol. Chem. 275*, 39678−39684.
7. Tang, M., Pham, P., Shen, X., Taylor, J. S., O'Donnell, M., Woodgate, R., and Goodman, M. F. (2000) Roles of E. coli DNA polymerases IV and V in lesion-targeted and untargeted SOS mutagenesis, *Nature 404*, 1014−1018.
8. Goodman, M. F., and Tippin, B. (2000) The expanding polymerase universe, *Nat. Rev. Mol. Cell Biol. 1*, 101−109.
9. Joyce, C. M., and Steitz, T. A. (1994) Function and structure relationships in DNA polymerases, *Annu. Rev. Biochem. 63*, 777−822.
10. Patel, P. H., and Loeb, L. A. (2001) Getting a grip on how DNA polymerases function, *Nat. Struct. Biol. 8*, 656−659.
11. Ling, H., Boudsocq, F., Woodgate, R., and Yang, W. (2004) Snapshots of replication through an abasic lesion; structural basis for base substitutions and frameshifts, *Mol. Cell 13*, 751−762.
12. Ling, H., Boudsocq, F., Woodgate, R., and Yang, W. (2001) Crystal structure of a Y-family DNA polymerase in action: a mechanism for error-prone and lesion-bypass replication, *Cell 107*, 91−102.
13. Nair, D. T., Johnson, R. E., Prakash, L., Prakash, S., and Aggarwal, A. K. (2005) Human DNA polymerase *ι* incorporates dCTP opposite template G via a G.C + Hoogsteen base pair, *Structure 13*, 1569−1577.
14. Cannistraro, V. J., and Taylor, J. S. (2007) Ability of Polymerase {eta} and T7 DNA Polymerase to Bypass Bulge Structures, *J. Biol. Chem. 282*, 11188−11196.
15. Garcia-Diaz, M., Bebenek, K., Krahn, J. M., Pedersen, L. C., and Kunkel, T. A. (2006) Structural analysis of strand misalignment during DNA synthesis by a human DNA polymerase, *Cell 124*, 331−342.
16. Kunkel, T. A., and Alexander, P. S. (1986) The base substitution fidelity of eucaryotic DNA polymerases. Mispairing frequencies, site preferences, insertion preferences, and base substitution by dislocation, *J. Biol. Chem. 261*, 160−166.
17. Kunkel, T. A. (1990) Misalignment-mediated DNA synthesis errors, *Biochemistry 29*, 8003−8011.
18. Kunkel, T. A., and Soni, A. (1988) Mutagenesis by transient misalignment, *J. Biol. Chem. 263*, 14784−14789.
19. Fowler, R. G., Degnen, G. E., and Cox, E. C. (1974) Mutational specificity of a conditional Escherichia coli mutator, mutD5, *Mol. Gen. Genet. 133*, 179−191.
20. Cai, H., Bloom, L. B., Eritja, R., and Goodman, M. F. (1993) Kinetics of deoxyribonucleotide insertion and extension at abasic template lesions in different sequence contexts using HIV-1 reverse transcriptase, *J. Biol. Chem. 268*, 23567−23572.
21. Efrati, E., Tocco, G., Eritja, R., Wilson, S. H., and Goodman, M. F. (1997) Abasic translesion synthesis by DNA polymerase *β* violates the "A-rule". Novel types of nucleotide incorporation by

human DNA polymerase β at an abasic lesion in different sequence contexts, *J. Biol. Chem. 272*, 2559−2569.
22. Baynton, K., Bresson-Roy, A., and Fuchs, R. P. (1999) Distinct roles for Rev1p and Rev7p during translesion synthesis in Saccharomyces cerevisiae, *Mol. Microbiol. 34*, 124−133.
23. Cordonnier, A. M., Lehmann, A. R., and Fuchs, R. P. (1999) Impaired translesion synthesis in xeroderma pigmentosum variant extracts, *Mol. Cell. Biol. 19*, 2206−2211.
24. Blanca, G., Villani, G., Shevelev, I., Ramadan, K., Spadari, S., Hubscher, U., and Maga, G. (2004) Human DNA polymerases λ and β show different efficiencies of translesion DNA synthesis past abasic sites and alternative mechanisms for frameshift generation, *Biochemistry 43*, 11605−11615.
25. Hamburgh, M. E., Curr, K. A., Monaghan, M., Rao, V. R., Tripathi, S., Preston, B. D., Sarafianos, S., Arnold, E., Darden, T., and Prasad, V. R. (2006) Structural determinants of slippage-mediated mutations by human immunodeficiency virus type 1 reverse transcriptase, *J. Biol. Chem. 281*, 7421−7428.
26. Delagoutte, E., Bertrand-Burggraf, E., Lambert, I. B., and Fuchs, R. P. (1996) Binding and incision activities of UvrABC excinuclease on slipped DNA intermediates that generate frameshift mutations, *J. Mol. Biol. 257*, 970−976.
27. Chi, L. M., and Lam, S. L. (2006) NMR investigation of DNA primer-template models: structural insights into dislocation mutagenesis in DNA replication, *FEBS Lett. 580*, 6496−6500.
28. Tissier, A., McDonald, J. P., Frank, E. G., and Woodgate, R. (2000) polι, a remarkably error-prone human DNA polymerase, *Genes Dev. 14*, 1642−1650.
29. Zhang, Y., Yuan, F., Wu, X., and Wang, Z. (2000) Preferential incorporation of G opposite template T by the low-fidelity human DNA polymerase ι, *Mol. Cell Biol. 20*, 7099−7108.
30. Johnson, R. E., Washington, M. T., Haracska, L., Prakash, S., and Prakash, L. (2000) Eukaryotic polymerases ι and ζ act sequentially to bypass DNA lesions, *Nature 406*, 1015−1019.
31. Hirao, I., Kawai, G., Yoshizawa, S., Nishimura, Y., Ishido, Y., Watanabe, K., and Miura, K. (1994) Most compact hairpin-turn structure exerted by a short DNA fragment, d(GCGAAGC) in solution: an extraordinarily stable structure resistant to nucleases and heat, *Nucleic Acids Res. 22*, 576−582.
32. Piotto, M., Saudek, V., and Sklenar, V. (1992) Gradient-tailored excitation for single-quantum NMR spectroscopy of aqueous solutions, *J. Biomol. NMR 2*, 661−665.
33. Sklenar, V., Piotto, M., Leppik, R., and Saudek, V. (1993) Gradient-Tailored Water Suppression for ^{1}H-^{15}N HSQC Experiments Optimized to Retain Full Sensitivity, *J. Magn. Reson. Ser. A 102*, 241−245.
34. Wüthrich, K. (1986) *NMR of Proteins and Nucleic Acids*, 1st ed., John Wiley & Sons, Inc., New York.
35. Altona, C., Faber, D. H., and Westra Hoekzema, A. J. A. (2000) Double-helical DNA ^{1}H chemical shifts: an accurate and balanced predictive empirical scheme, *Magn. Reson. Chem. 38*, 95−107.
36. Peyret, N., Seneviratne, P. A., Allawi, H. T., and SantaLucia, J., Jr. (1999) Nearest-neighbor thermodynamics and NMR of DNA sequences with internal A. A, C. C, G. G, and T. T mismatches, *Biochemistry 38*, 3468−3477.
37. Ornstein, R. L., Rein, R., Breen, D. L., and MacElroy, R. D. (1978) An optimized potential function for the calculation of nucleic acid interaction energies I. Base stacking, *Biopolymers 17*, 2341−2360.
38. Gaffney, B. L., and Jones, R. A. (1989) Thermodynamic comparison of the base pairs formed by the carcinogenic lesion O6-methylguanine with reference both to Watson-Crick pairs and to mismatched pairs, *Biochemistry 28*, 5881−5889.
39. Ke, S. H., and Wartell, R. M. (1993) Influence of nearest neighbor sequence on the stability of base pair mismatches in long DNA; determination by temperature-gradient gel electrophoresis, *Nucleic Acids Res. 21*, 5137−5143.
40. Lam, S. L. (2007) DSHIFT—a web server for predicting DNA chemical shifts. *Nucleic Acids Res.*, 10.1093/nar/gkm320.

BI700865E